Available online at www.sciencedirect.com
SCIENCE DIRECT®
Computational Materials Science 32 (2005) 268–275
COMPUTATIONAL MATERIALS SCIENCE
www.elsevier.com/locate/commatsci

Thermo-plasticity of metal foams

S. Benke *, D. Weichert [1]

Institute of General Mechanics, RWTH Aachen, Aachen, Germany

Abstract

The thermo-mechanical behaviour of a fluid-filled metal foam is influenced by the characteristics of the solid skeleton and the pore-fluid. During the deformation process both constituents exchange momentum and energy. Based on the theory of porous media a fluid-filled foam is modeled as a binary mixture consisting of a metal skeleton and a pore-gas. The porous solid skeleton is assumed to behave thermo-elasto-plastically. The pore-gas is considered as an ideal gas. For both constituents different phase temperatures and thermo-mechanical coupling mechanisms are taken into account. The resulting system of differential equations is solved using the finite element method. An example demonstrates the applicability and validity of this approach.

PACS: 46.15.Cc
Keywords: Porous media; Finite element method; Thermo-plasticity; Multi-physics

1. Introduction

The development of new metal foams made of stainless steel enables their application in heat exchanger components or effusion cooled multi-layer systems in power plants [1,2]. The thermo-mechanical behaviour of fluid-filled porous structures is determined by the characteristics of the solid phase, the fluid phase and the exchange processes between both constituents. From an engineering point of view the exact modeling of the statistical pore structure on the micro-scale is not possible due to its complexity and due to the fact that the exact pore geometry mostly remains unknown. A well established thermodynamically consistent macroscopical framework for the modeling of fluid-filled porous solids is given by the theory of porous media [3–5]. The basic idea of the theory of porous media is the concept of superimposed continua as it is used by mixture theories combined with the concept of volume fractions [6,7].

The thermo-mechanical coupling processes in fluid-filled porous media are quite complex. In

* Corresponding author. Address: ACCESS e.V., Aachen, Germany.
E-mail address: s.benke@access.rwth-aachen.de (S. Benke).
[1] Present address: INSA Rouen, France.

0927-0256/$ - see front matter © 2004 Elsevier B.V. All rights reserved.
doi:10.1016/j.commatsci.2004.09.042

each phase the thermo-mechanical coupling is two-fold: on the one hand, changes of the temperature lead to volumetric deformation of the medium due to thermal expansion or contraction. On the other hand, the deformation of ductile solids lead to temperature changes due to thermo-elastic and dissipative plastic effects. The volumetric compression or expansion of a gas also leads to temperature changes. The different constituents in the porous medium interact with each other through the exchange of momentum and energy.

In this article the foam is treated as a two-phase model consisting of a porous metal skeleton saturated by a compressible pore-gas. For both constituents different motion functions are considered. Since the heat generation in both phases due to the thermo-mechanical coupling effects is different, the assumption of a local thermal equilibrium between the phases is not possible [8]. Therefore, different phase temperatures are taken into account. The transfer of mass between the phases is neglected. Using this model the thermo-mechanical coupling processes in low-density metal foams are studied by numerical simulation.

The theoretical background of porous media models is well understood in the last years but their numerical simulation is still a delicate task. One reason is the increasing number of primary field variables in models using an approach of superimposed continua. In our binary model the solid displacement, the pore pressure and the solid and fluid temperature are the primary unknowns. On the other hand the multiple physical effects included in the model give rise to a complex system of differential equations. The introduced coupling mechanisms and the nonlinear material behaviour lead to a complex system of differential equations to be solved by the finite element method. During the solution procedure several numerical difficulties arise.

2. A porous media model with different phase temperatures

In this section we briefly introduce the governing equations of the model: the kinematic relations, the concept of volume fractions, the balance equations and the constitutive material laws. For further details on the history and the theoretical foundations of the theory of porous media, we refer to de Boer et al. [9] and Ehlers [10].

2.1. Kinematics

In the framework of the theory of porous media, the fluid-filled porous metal foam is considered as a mixture of the immiscible constituents solid skeleton φ^{S} and pore fluid φ^{F}. This means, each point x in the current configuration at time t is simultaneous occupied by the material points X^{α} of all constituents φ^{α} which proceed from different reference positions X^{α}. To each constituent an individual motion function is assigned:

$$x = \chi_{\alpha}(X_{\alpha}, t). \tag{1}$$

With the help of the motion function the phase velocities and the deformation measures are defined as usual in continuum mechanics. In our case, the solid skeleton builds the reference frame for the deformation of the whole porous body. The description of the fluid motion makes use of a modified Eulerian formulation relative to the solid skeleton. The fluid flow through the deformable solid skeleton is characterized by the relative velocity v_{FS}:

$$v_{FS} = v_{F} - (u_{S})'_{S}. \tag{2}$$

Here, v_{F} is the velocity of φ^{F} and $(\cdot)'_{S} = \hat{\partial}(\cdot)/\partial t + \operatorname{grad}(\cdot)\dot{x}_{\alpha}$ denotes the material derivative of the constituent φ^{α}. Furthermore, the operator "grad(·)" is the partial derivative of (·) with respect to the current position x. The displacement vector of the solid is denoted by u_{S}.

In order to formulate the volume fraction concept, the existence of the volume fraction n^{α}:

$$n^{\alpha} = n^{\alpha}(x, t) = \frac{\mathrm{d}v^{\alpha}}{\mathrm{d}v} \tag{3}$$

is assumed. The volume fraction n^{α} can be considered as a scalar structure variable. It is defined as the ratio of the constituent volume $\mathrm{d}v^{\alpha}$ and the bulk volume $\mathrm{d}v$. Thus, in absence of any vacant space, the saturation condition yields:

$$n^{S} + n^{F} = 1. \tag{4}$$

Associated with the volume fraction concept is the introduction of the bulk density ρ^α and the partial density $\rho^{\alpha R}$:

$$\rho^\alpha = n^\alpha \rho^{\alpha R}. \tag{5}$$

2.2. Balance equations

In the framework of a thermo-mechanical theory of multi-phase materials, the local field equations are the balance of mass, the balance of momentum and the balance of energy. Restricting the considerations to quasi-static processes without mass exchange between the phases and without external heat supply the balance equations read [3,5,10]:

- balance of mass:

$$(\rho^\alpha)'_\alpha + \rho^\alpha \operatorname{div} \boldsymbol{v}_\alpha = 0, \tag{6}$$

- balance of momentum:

$$\operatorname{div} \boldsymbol{\sigma}^\alpha + \rho^\alpha \boldsymbol{b} = \hat{\boldsymbol{p}}^\alpha, \tag{7}$$

- balance of energy:

$$\rho^\alpha[(\psi^\alpha)'_\alpha + (\vartheta^\alpha)'_\alpha s^\alpha + \vartheta^\alpha (s^\alpha)'_\alpha] - \boldsymbol{\sigma}^\alpha \boldsymbol{D}_\alpha + \operatorname{div} \boldsymbol{q}^\alpha = -\hat{e}^\alpha + \hat{\boldsymbol{p}}^\alpha \boldsymbol{v}_\alpha. \tag{8}$$

In these relations, "div(·)" denotes the divergence operator with respect to the current position, $\boldsymbol{\sigma}^\alpha$ is the symmetric Cauchy stress tensor and $\boldsymbol{D}_\alpha$ is the strain rate of the constituent φ^α. Furthermore, ψ^α is the specific free Helmholtz-energy, and ϑ^α the phase-temperature. The specific entropy is denoted by s^α and the heat flux vector by $\boldsymbol{q}^\alpha$. In the momentum balance (7) it has been assumed that $\boldsymbol{b} = \boldsymbol{b}^\alpha$ is the overall volumetric force per unit mass acting on all constituents. The quantities $\hat{\boldsymbol{p}}^\alpha$ and $\hat{e}^\alpha$ represent the interaction terms for momentum and energy. They are constrained by

$$\hat{\boldsymbol{p}}^S + \hat{\boldsymbol{p}}^F = 0 \tag{9}$$

and

$$\hat{e}^S + \hat{e}^F = 0, \tag{10}$$

since no momentum and energy production takes place in the porous medium.

2.3. Constitutive settings

As a result of the assumption of a material incompressible solid skeleton ($\rho^{SR} = \text{constant}$) and a compressible pore fluid (hybrid model of the second type) the expressions for the stress tensors and the interaction force read [11]:

$$\boldsymbol{\sigma}^S = -n^S p \frac{\vartheta^S}{\vartheta^F} \boldsymbol{I} + \boldsymbol{\sigma}^S_E, \tag{11}$$

$$\boldsymbol{\sigma}^F = -n^F p \boldsymbol{I} + \boldsymbol{\sigma}^F_E. \tag{12}$$

The tensor $\boldsymbol{I}$ is the identity tensor. Here, the first terms are a consequence of the evaluation of the entropy inequality, using the volume balance as a constraint for the whole deformation process of the porous body. The extra terms $(\cdot)^\alpha_E$ are governed by the deformation of the constituents and the flow of the pore-fluid [5].

In this article we neglect the extra stress in the gaseous pore fluid $\boldsymbol{\sigma}^F_E$. This term is assumed to be small compared to the viscous momentum interaction force $\hat{\boldsymbol{p}}^F$ [12]:

$$\hat{\boldsymbol{p}}^F = \beta_p(\vartheta^F - \vartheta^S) - \frac{(n^F)^2 \gamma^{FR}}{k^S} \boldsymbol{v}_{FS} + p \frac{\vartheta^F + \vartheta^S}{2\vartheta^S} \operatorname{grad} n^F. \tag{13}$$

Here, k^S is the permeability of the solid skeleton and γ^{FR} the effective shear viscosity of the pore fluid, whereas β_p describes the influence of the temperature difference between the phases on the momentum interaction. For quasi-static flow processes, neglecting the thermal influence on the momentum interaction force $\hat{\boldsymbol{p}}^F$, Eq. (13) leads to the well known *Darcy* law:

$$n^F \boldsymbol{v}_{FS} = \frac{k^S}{\gamma^{FR}} (\operatorname{grad} p - \rho^{FR} \boldsymbol{b}). \tag{14}$$

The permeability k^S of the solid skeleton depends strongly on the structure of the pores and thus on the deformation state of the solid skeleton. In our case we assume a linear relationship between the permeability and the fluid volume fraction n^F:

$$k^F(n^F) = k^F_0 \left(\frac{n^F}{n^F_0} \right). \tag{15}$$

For an initial fluid fraction n_0^F the permeability is given by k_0^F.

Following the geometrically nonlinear approach in thermo-elasto-plasticity, the deformation gradient of the solid skeleton $\boldsymbol{F}_S$ is multiplicatively decomposed into thermal $(\cdot)_{S\vartheta}$, elastic $(\cdot)_{Se}$ and plastic $(\cdot)_{Sp}$ parts [13]:

$$\boldsymbol{F}_S = \boldsymbol{F}_{S\vartheta}\boldsymbol{F}_{Se}\boldsymbol{F}_{Sp}. \tag{16}$$

This leads to an additive decomposition of the Green deformation tensor $\boldsymbol{E}_S$:

$$\boldsymbol{E}_S = \boldsymbol{E}_{S\vartheta} + \boldsymbol{E}_{Se} + \boldsymbol{E}_{Sp}. \tag{17}$$

The extra stresses of the solid are governed by the St. Venant-Kirchhoff law:

$$\boldsymbol{S}_E^S = \lambda(\boldsymbol{E}_{Se}\boldsymbol{I})\boldsymbol{I} + 2\mu\boldsymbol{E}_{Se}, \tag{18}$$

where μ and λ are the effective Lamé constants of the solid skeleton. In order to describe the plastic material behaviour, we introduce a simple yield function for the metal skeleton developed by Deshpande and Fleck [14]:

$$F = \sqrt{\frac{\sigma_{Sv}^2 - \beta_a^2\sigma_{Sh}^2}{1 + (\beta_a/3)^2}} - Y^S = 0, \tag{19}$$

which is very similar to a flow rule given previously by Green [15]. In Eq. (19) σ_{Sh} and σ_{Sv} are the hydrostatic and the von Mises parts of the extra stress $\boldsymbol{\sigma}_E^S$ in the solid skeleton. The material parameter β_a weights the influence of the hydrostatic stress on the yield behaviour. Y^S is the yield limit of the solid skeleton. We adopt isotropic strain hardening:

$$Y = Y_0 + R(P), \tag{20}$$

where Y_0 is the initial yield limit and R is a function of the accumulated effective plastic strain P of the solid material. As proposed by Deshpande and Fleck, we assume associated plasticity:

$$\boldsymbol{D}_{Sp} = \Lambda\frac{\partial F}{\partial\boldsymbol{\sigma}_E^S}, \tag{21}$$

where $\boldsymbol{D}_{Sp}$ is the plastic strain rate of the solid material and Λ is the plastic multiplier.

In the case of small temperature variations, the increment of thermal deformation $\Delta\boldsymbol{E}_{S\vartheta}$ due to the temperature variation $\Delta\vartheta^S$ is given by the linear thermal expansion law:

$$\Delta\boldsymbol{E}_{S\vartheta} = \alpha_s\boldsymbol{I}\Delta\vartheta^S. \tag{22}$$

Here, α_s denotes the isotropic thermal expansion coefficient. Investigations on the thermal transport in metal foams have shown that the heat transfer is dominated by the conductivity of the solid skeleton [16]. Thus, we assume the validity of the Fourier law:

$$\boldsymbol{q}^S = -\lambda^S\operatorname{grad}\vartheta^S. \tag{23}$$

The effective thermal conductivity λ^S includes the solid to solid heat transfer due to radiation via a transparent gas. The isochor heat capacity of the solid is given by c_v^{SR}. The plastic work of the solid skeleton leads to heat generation caused by dissipative plastic effects:

$$r_{Sp} = \eta\boldsymbol{\sigma}^S : \boldsymbol{D}_{Sp}. \tag{24}$$

The parameter η defines the portion of the plastic work which is dissipated as heat. It is assumed that the remaining portion of the plastic work is stored within the material, raising the internal energy. Because of the specific elastic deformation mechanism of metal foams, which is based on bending of the foam cell struts, the thermo-elastic coupling effects are neglected in our macroscopic model.

The pore-gas is considered as an ideal gas. The pressure p is related to the temperature ϑ^F and the real density ρ^{FR} of the fluid phase by

$$p = R\rho^{FR}\vartheta^F. \tag{25}$$

Since the solid skeleton defines the frame of reference for the deformation process, the heat flux in the fluid consists of a conductive and a convective term:

$$\boldsymbol{q}_{res}^F = -\lambda^F\operatorname{grad}\vartheta^F + \rho^F c_v^F\boldsymbol{v}_{FS}\operatorname{grad}\vartheta^F. \tag{26}$$

Here, c_v^F is the heat capacity of the gas.

Beside the constitutive setting for the material behaviour, the energy exchange still has to be quantified. We postulate that the energy transfer is a function of the temperature difference only:

$$\hat{e}^F - \hat{\boldsymbol{p}}^F\cdot\boldsymbol{v}_S = -\alpha_q(\vartheta^F - \vartheta^S). \tag{27}$$

The heat transfer coefficient α_q in general depends on the relative velocity $\boldsymbol{v}_{FS}$ of the fluid flow.

3. Numerical discretization

The discrete numerical model is derived within three steps:

- The balance equations are modified and transformed into a variational form. This establishes the basis for the following numerical discretization.
- The discretization in space is carried out by inserting suitable finite elements. Here, we make use of extended Taylor–Hood elements. The solid displacement $\boldsymbol{u}$, the pressure p and the temperatures ϑ^{S} and ϑ^{F} are the primary field variables.
- The time-continuous model is then discretized in time by the use of a semi-implicit Euler method.

3.1. Variational formulation

Let $\mathscr{B} \subset \mathbb{R}^3$ be the current configuration, and $\partial\mathscr{B}_u \subset \partial\mathscr{B}$, $\partial\mathscr{B}_{\mathrm{p}} \subset \partial\mathscr{B}$ and $\partial\mathscr{B}_\vartheta \subset \partial\mathscr{B}$ the boundary parts, where we describe the Dirichlet boundary conditions for the solid displacement $\boldsymbol{u} = \bar{\boldsymbol{u}}$, the fluid pressure $p = \bar{p}$ and the phase temperatures $\vartheta^\alpha = \bar{\vartheta}^\alpha$.

Combining the balance of momentum (7) for solid and fluid, (11) and (12), we obtain:

$$-\int_{\mathscr{B}} \left(\left(\frac{n^{\mathrm{S}}\vartheta^{\mathrm{S}}}{\vartheta^{\mathrm{F}}} + n^{\mathrm{F}} \right) p\boldsymbol{I} \right) : \operatorname{grad} \boldsymbol{u}^\star \,\mathrm{d}v + \int_{\mathscr{B}} (\boldsymbol{\sigma}^{\mathrm{S}}_{\mathrm{E}}) : \operatorname{grad} \boldsymbol{u}^\star \,\mathrm{d}v = \mathscr{L}_1 \tag{28}$$

for all test functions $\boldsymbol{u}^\star$ satisfying $\boldsymbol{u}^\star = 0$ on $\partial\mathscr{B}_u$. The vector $\mathscr{L}_1$ containing the body forces and surface loads on $\partial\mathscr{B}_t$ is given by

$$\mathscr{L}_1 = \int_{\mathscr{B}} (\rho^{\mathrm{S}} + \rho^{\mathrm{F}}) \boldsymbol{b}\boldsymbol{u}^\star \,\mathrm{d}v + \int_{\partial\mathscr{B}_t} \boldsymbol{t}\boldsymbol{u}^\star \,\mathrm{d}a. \tag{29}$$

The balance of mass for the porous body is a combination of the individual mass balance equations (6), the saturation condition (4) and the definition of the momentum exchange (13). Assuming $\beta_{\mathrm{p}} = 0$, we obtain:

$$\int_{\mathscr{B}} \left(\operatorname{div}((\boldsymbol{u})'_{\mathrm{S}}) + \frac{\partial \rho^{\mathrm{F}}}{\rho^{\mathrm{F}} \partial t} \right) p^\star \,\mathrm{d}v + \int_{\mathscr{B}} \frac{k^{\mathrm{F}}}{\gamma^{\mathrm{FR}}} \operatorname{grad} p \operatorname{grad} p^\star \,\mathrm{d}v = \mathscr{L}_2, \tag{30}$$

simplifying the general fluid flow relation to a potential formulation. The test function $p^\star$ must satisfy $p^\star = 0$ on $\partial\mathscr{B}_{\mathrm{p}}$. The body forces and the prescribed fluid flow are given by $\mathscr{L}_2$:

$$\mathscr{L}_2 = \int_{\mathscr{B}} \rho^{\mathrm{FR}} \boldsymbol{b} \operatorname{grad} p^\star \,\mathrm{d}v + \int_{\partial\mathscr{B}_j} v_{\mathrm{FS}} \boldsymbol{n} p^\star \,\mathrm{d}a. \tag{31}$$

For the thermal subproblem we need to evaluate the variational form of the heat transfer equation for both constituents. Based on balance of energy (8) we obtain the coupled heat transfer equation of the deformable thermo-elastic–plastic solid skeleton:

$$\int_{\mathscr{B}} (\rho^{\mathrm{S}} c_v^{\mathrm{S}} \dot{\vartheta}^{\mathrm{S}}) \vartheta^\star_{\mathrm{S}} - \boldsymbol{q}^{\mathrm{S}} \operatorname{grad} \vartheta^\star_{\mathrm{S}} \,\mathrm{d}v = \mathscr{L}_3, \tag{32}$$

where the test function $\vartheta^\star_{\mathrm{S}}$ must satisfy $\vartheta^\star_{\mathrm{S}} = 0$ on $\partial\mathscr{B}_\vartheta$. The heat supply due to the boundary condition on $\partial\mathscr{B}_q$, the dissipated plastic work and the heat transfer between solid and fluid is defined by $\mathscr{L}_3$:

$$\mathscr{L}_3 = \int_{\mathscr{B}} (r_{\mathrm{Sp}} - \hat{e}^{\mathrm{F}}) \vartheta^\star_{\mathrm{S}} \,\mathrm{d}v - \int_{\partial\mathscr{B}_q} q^{\mathrm{S}}_n \vartheta^\star_{\mathrm{S}} \,\mathrm{d}a. \tag{33}$$

Combining the balance of energy for the fluid (8) and the state equation of the ideal gas (25), we obtain the fluid heat transfer equation:

$$\int_{\mathscr{B}} (\rho^{\mathrm{F}} c_v^{\mathrm{F}} \dot{\vartheta}^{\mathrm{F}} - p \operatorname{tr} \boldsymbol{D}_{\mathrm{F}}) \vartheta^\star_{\mathrm{F}} \,\mathrm{d}v + \int_{\mathscr{B}} (-\boldsymbol{q}^{\mathrm{F}}) \operatorname{grad} \vartheta^\star_{\mathrm{F}} \,\mathrm{d}v = \mathscr{L}_4 \tag{34}$$

for all test functions $\vartheta^\star_{\mathrm{F}}$ satisfying $\vartheta^\star_{\mathrm{F}} = 0$ on $\partial\mathscr{B}_\vartheta$, with:

$$\mathscr{L}_4 = \int_{\mathscr{B}} (\hat{e}^{\mathrm{F}}) \vartheta^\star_{\mathrm{F}} \,\mathrm{d}v - \int_{\partial\mathscr{B}_q} q^{\mathrm{F}}_n \vartheta^\star_{\mathrm{F}} \,\mathrm{d}a. \tag{35}$$

The variational equations are completed by the several constitutive equations.

3.2. Discretization in space and time

The resulting system of partial differential equations is solved with the help of the finite element

method. The primary unknowns are the displacement of the solid, the pore pressure and the solid and fluid temperature. This leads to a formulation using (dim + 3) primary field variables, where dim is the dimension of the chosen finite element. For the discretization in space, solution we use extended Taylor–Hood elements as shown in Fig. 1. The solid displacement field is approximated by quadratic shape functions. For the pressure field and the temperature fields linear shape functions are used. The numeric integration is carried out with a full Gauß quadrature using 27 integration points on hexahedron elements.

The time continuous system of differential equations is then discretized in time by a semi-implicit Euler method. Due to the nonlinearity of the differential equations, a solution for the displacements $\boldsymbol{u}$, the pressure p and the temperatures ϑ^{α} has to be computed iteratively in each time step $\Delta t = t_n - t_{n-1}$ of the considered interval $[t_0; t_N]$. Therefore, an updated Lagrange an approach combined with a Newton process is used. To obtain a reasonable convergence rate, we introduce a consistent tangent operator.

The heat generation due to the dissipative plastic effects and the heat transfer between the phases is taken into account by a staggered solution method. After evaluating the secondary field variables plastic strain, solid stress and fluid velocity, we calculate the heat flux given in the first term of Eq. (33). Since the time discretization is reasonably high an explicit solution method is used to take these heat fluxes into account. Numerical investigations show that this leads to a stable and accurate algorithm.

4. Numerical simulation

In the following the results are presented for the crushing of a box filled with a closed-cell low-density aluminium foam as shown in Fig. 2. This example is realized with the help of the finite element code PARFEM. The material parameters of the solid skeleton given in Table 1 are based on published experimental results of a commercial aluminium foam [14,17]. The properties of the pore-gas are defined by air at normal conditions [18]. The box is compressed by a pre-described velocity v_0 on the upper surface of the foam box. The deformation process is assumed to be adiabatic.

Fig. 3 displays the evolution of the solid volume fraction with respect to the normalized displacement $\bar{u} = u/L$. Fig. 4 shows the stress in loading direction in the solid skeleton and the pressure in the fluid phase. The change of temperature in the solid skeleton due to dissipative plastic effects is very small because of the low yield strength and the low hardening behaviour of the foam (Fig. 5). In contrast, the thermo-mechanical coupling effects in the pore gas are much stronger. The numerical results shown in Fig. 6 follow the analytical solution of adiabatic compression with reasonable accuracy. As a result of the study, the pore gas needs to be included in the thermo-mechanical

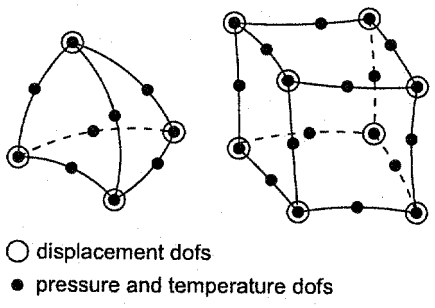

Fig. 1. Nodal points of extended Taylor–Hood tetrahedron and hexahedron elements.

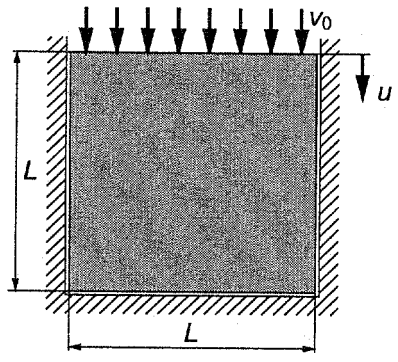

Fig. 2. Sketch of the compression test.

Table 1
Properties of the solid skeleton

Parameter	Symbol	Value (SI-units)
Lamé constants	μ	4.65×10^4
	λ	0.0
Effective density	ρ^{SR}	7.84×10^4
Yield criterion	Y	4.9
	β_a	$\sqrt{9/2}$
Thermal expansion	α	1.0×10^{-6}
Thermal conductivity	λ	9.961
Heat capacity	c^{SR}	8.88×10^2
Plastic dissipation	η	0.9
Permeability	k^F	∞
	β_p	0.0
Heat transfer	α_q	0.0

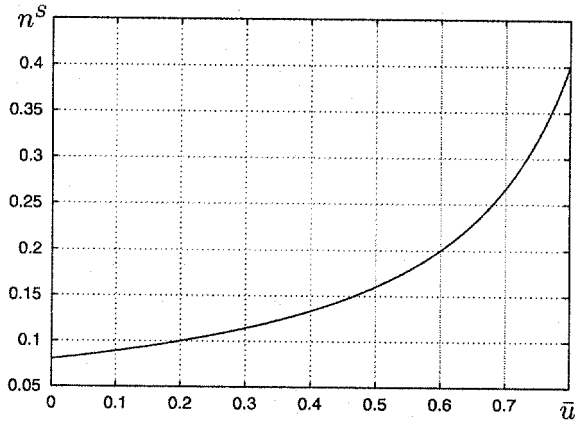

Fig. 3. Evolution of the solid volume fraction n^S.

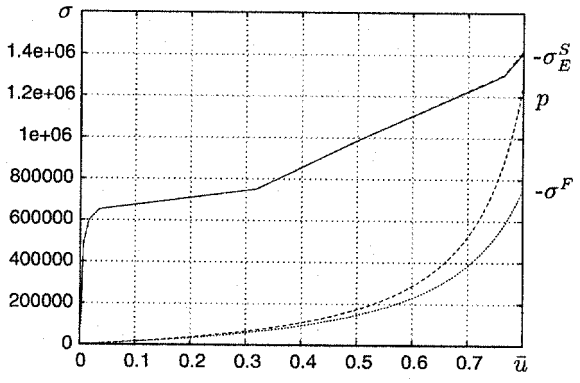

Fig. 4. Stresses in the constituents.

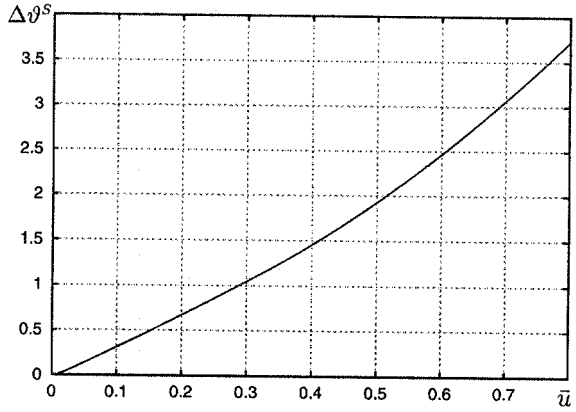

Fig. 5. Temperature change in the solid.

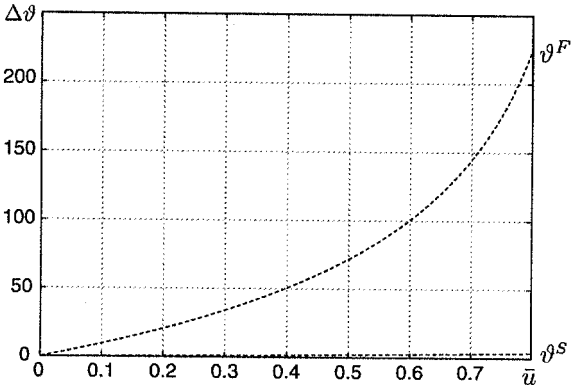

Fig. 6. Temperature changes in the constituents.

modeling of low-density metal foams. Models found in literature which neglect the pore fluid may therefore underestimate the thermal effects of a mechanical deformation [17].

5. Conclusion

In the present paper the thermo-mechanical coupling processes in a fluid-filled metal foam are modeled on the macro-scale using the theory of porous media. The example calculation shows that the basic coupling mechanisms can be described correctly. For a gas-filled low-density aluminium foam the calculations indicate that the thermo-mechanical coupling effects in the pore-gas are much stronger than in the solid skeleton. Presently

used thermo-mechanical models which neglect the influence of the fluid therefore underestimate the thermal effects of the deformation process.

References

[1] U. Mohr, W. Bleck, P.-F. Scholz, Herstellung von offenporigem Metallschaum über den SchlickerReaktions-SchaumSinter-Prozess, in: Proceedings 17, Aachener Stahlkolloquium Werkstofftechnik "Perspektiven mit Stahl", 23–24 May 2002, Aachen, 2002, pp. 245–254.

[2] SFB 561, Thermisch hochbelastete, offenporige und gekühlte Mehrschichtsysteme für Kombi-Kraftwerke: Arbeits- und Ergebnisbericht, Technical report, RWTH Aachen, 2003.

[3] R.M. Bowen, Theory of mixtures, in: C. Eringen (Ed.), Continuum Physics, Academic Press, New York, 1976, pp. 1–127.

[4] R. de Boer, W. Ehlers, On the problem of fluid- and gas-filled elasto-plastic solids, Int. J. Solids Struct. 22 (1986) 1231–1241.

[5] R. de Boer, Theory of Porous Media, Springer-Verlag, Berlin, New York, 2000.

[6] C. Truesdell, R. Toupin, The classical field theories, in: S. Flügge (Ed.), vol. III/1., Handbuch der Physik, Springer-Verlag, Berlin, 1960.

[7] R.M. Bowen, Incompressible porous media models by use of the theory of mixtures, Int. J. Eng. Sci. 18 (1980) 1129–1148.

[8] M. Kaviany, Principles of Heat Transfer in Porous Media, second ed., Springer-Verlag, Berlin, 1995.

[9] R. de Boer, J. Bluhm, J. Skolnik, Allgemeine Plastizitätstheorie für poröse Medien, Forschungsbericht aus dem fachbereich bauwesen, Universität-Gesamthochschule Essen, November 1996.

[10] W. Ehlers, Poröse Medien: Ein Kontinuumsmechanisches Modell auf der Basis der Mischungstheorie, Habilitationsschrift, Universität-Gesamthochschule Essen, 1989.

[11] J. Bluhm, Modeling of saturated thermo-elastic porous solids with different phase temperatures, in: W. Ehlers, J. Bluhm (Eds.), Porous Media: Theory, Experiments and Numerical Applications, Springer-Verlag, Berlin, 2002.

[12] S. Diebels, W. Ehlers, B. Markert, Neglect of the fluid extra stresses in volumetrically coupled solid–fluid problems, ZAMM 81 (2001) 521–522.

[13] C. Miehe, Zur numerischen Behandlung thermomechanischer Prozesse, Dissertation, Universität Hannover, Forschungs- und Seminarberichte aus dem Bereich der Mechanik der Universität Hannover, Bericht-Nr. 88/6, Hannover, 1988.

[14] V.S. Deshpande, N.A. Fleck, Isotropic constitutive models for metallic foams, J. Mech. Phys. Solids 48 (6–7) (2000) 1253–1283.

[15] R.J. Green, A plasticity theory for porous solids, Int. J. Mech. Sci. 14 (1972) 215–224.

[16] K. Boomsma, D. Poulikakos, On the effective thermal conductivity of a three dimensionally structured fluid-saturated metal foam, Int. J. Heat Mass Transfer 44 (2001) 827–836.

[17] A. Rabiei, A.G. Evans, J.W. Hutchinson, Heat generation during the fatigue of a cellular Al alloy, Metall. Mater. Trans. 31A (4) (2000) 1129–1136.

[18] H.D. Baehr, Thermodynamik, third ed., Springer-Verlag, Berlin, 1973.